



LAWRENCE
LIVERMORE
NATIONAL
LABORATORY

Near-Infrared Spectroscopy for Divertor Plasma Diagnosis and Control in DIII-D tokamak

V. A. Soukhanovski, A. G. McLean, S. L. Allen

June 2, 2014

20th Topical Conference on High-Temperature Plasma
Diagnostics (HTPD 2014)
Atlanta, GA, United States
June 1, 2014 through June 5, 2014

Disclaimer

This document was prepared as an account of work sponsored by an agency of the United States government. Neither the United States government nor Lawrence Livermore National Security, LLC, nor any of their employees makes any warranty, expressed or implied, or assumes any legal liability or responsibility for the accuracy, completeness, or usefulness of any information, apparatus, product, or process disclosed, or represents that its use would not infringe privately owned rights. Reference herein to any specific commercial product, process, or service by trade name, trademark, manufacturer, or otherwise does not necessarily constitute or imply its endorsement, recommendation, or favoring by the United States government or Lawrence Livermore National Security, LLC. The views and opinions of authors expressed herein do not necessarily state or reflect those of the United States government or Lawrence Livermore National Security, LLC, and shall not be used for advertising or product endorsement purposes.

Near-infrared Spectroscopy for Divertor Plasma Diagnosis and Control in DIII-D Tokamak^{a)}

V. A. Soukhanovskii,^{1, b)} A. G. McLean,¹ and S. L. Allen¹

Lawrence Livermore National Laboratory, Livermore, California

Divertor recycling and low- Z impurity flux measurements, a spectral survey for divertor Thomson scattering (DTS) diagnostic, and a T_e monitor for divertor detachment control are proposed based on the new near infrared (NIR) emission measurements performed in the DIII-D tokamak divertor plasma. A commercial 0.3 m spectrometer coupled to an imaging lens via optical fiber and a InGaAs 1024 pixel array detector enabled deuterium and impurity emission measurements in the range 800 - 2300 nm. The first full NIR survey identified D, He, B, Li, C, N, O, Ne lines and provided plasma T_e , n_e estimates from deuterium Paschen series intensity and Stark line broadening analysis. The range 1.000-1.060 μm was surveyed during high-density and neon seeded divertor operation for spectral background emission studies for $\lambda = 1.064 \mu\text{m}$ laser-based DTS development. The ratio of adjacent deuterium Paschen- α and Brackett Br9 lines in recombining divertor plasmas is proposed for divertor T_e estimates aimed at divertor detachment real-time feedback control.

Keywords: near infrared, spectroscopy, divertor, detachment, impurities, Stark

^{a)}Contributed paper published as part of the Proceedings of the 20th Topical Conference on High-Temperature Plasma Diagnostics, Atlanta, Georgia, June, 2014.

^{b)}Electronic mail: vlad@llnl.gov

I. INTRODUCTION

To date, the near-infrared (NIR, 750-2300 nm) spectral region has not been extensively used for fusion plasma diagnostics. Based on measurements in the NSTX tokamak divertor several diagnostic applications have been proposed for plasma control and performance measurements in the burning plasma nuclear fusion device¹⁻³. While NIR spectroscopic systems share instrumental concepts with the ultraviolet and visible spectroscopy, NIR optical material and component properties are much more tolerant to nuclear radiation and plasma effects, and NIR signal extraction and detection techniques are mature².

A recent NIR emission survey of the DIII-D tokamak divertor plasma extended the upper wavelength limit to 2300 nm by taking advantage of a specialized InGaAs array detector, in comparison with our previous survey in NSTX where a conventional silicon CCD detector limited the upper wavelength to 1100 nm. In this work we focus on three new aspects resulting from the extended NIR spectral measurements in the DIII-D divertor. First, a first of a kind survey from 800 to 2300 nm identified a full deuterium Paschen $n = 3 - m, m = 4...12$ series lines, and a number of low- Z impurity lines that can be used for recycling and impurity flux measurements. Second, we performed high spectral resolution measurements in the region $1.000 - 1.064 \mu\text{m}$ to study the background and line emissions in the range relevant to the performance of a divertor Thomson scattering (DTS) system based on a Nd:YAG laser with $\lambda = 1.064 \mu\text{m}$. And third, for the first time we identified the Brackett series lines $n = 5 - m, m = 9...11$ resulting from recombination. Measurements of the T_e -sensitive Paschen- α and Brackett line intensity ratios are proposed for radiative divertor feedback control.

II. EXPERIMENT AND METHOD

DIII-D tokamak is a large tokamak with graphite plasma-facing components, featuring high-performance deuterium plasmas that result in intense particle and heat fluxes in the divertor⁴. The measurements were performed using a commercial 0.3 m spectrograph and an InGaAs array detector. The Acton Research Corporation Model SP300i spectrograph was equipped with two replica NIR-capable gratings: 1200 line/mm and 300 lines/mm, both blazed at 500 nm. The detector, a Princeton Instruments Model OMA V array with

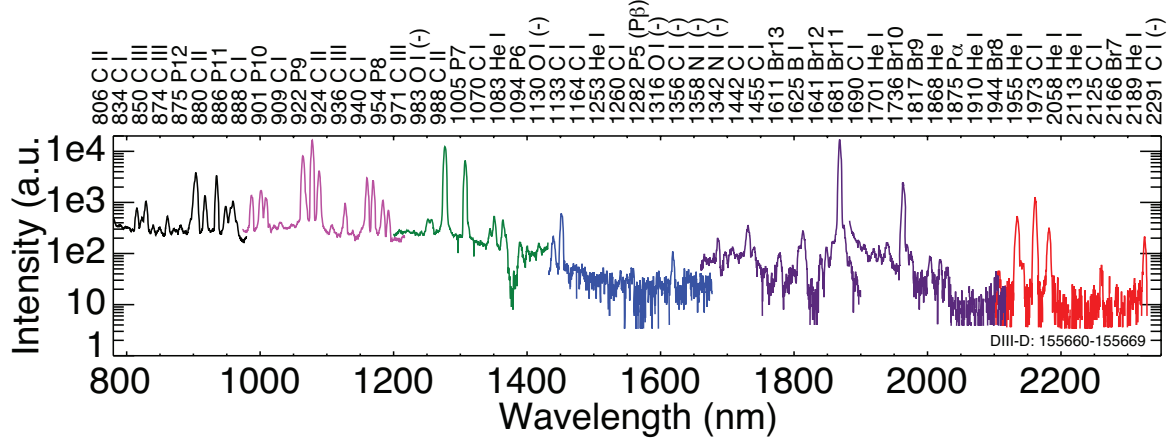


FIG. 1. Divertor survey spectrum. The series lines are labeled by the series letter and the number of the upper n level, e.g., P7 for the Paschen line corresponding to the $n = 7 - 3$ transition. The lines absent in ADAS are labeled with "(-)".

1024 tall pixels ($25 \times 250 \mu\text{m}$) provided 16-bit digitization at 1 MHz, i.e., up to 900 scans per second. The OMA V array had liquid nitrogen cooling. With the higher spectral resolution 1200 l/mm grating measurements between 800 and 1500 nm were possible with $\lambda/\delta\lambda \sim 1200$, while the lower resolution 300 l/mm grating enabled survey spectra up to the detector sensitivity limit at about $2.3 \mu\text{m}$ with a lower resolution $\lambda/\delta\lambda \sim 200 - 400$. A $10 \mu\text{m}$ entrance slit width was used. The spectrometer was coupled by existing optical fibers to imaging lenses mounted on DIII-D tokamak window ports. The existing fibers were not NIR-optimized, resulting in reduced intensity regions in recorded spectra. Two types of fiber views were used: a tangential divertor line of sight of the inner divertor leg region, and a radial line of sight co-linear with DTS fibers and intersecting the inner and (or) the outer divertor legs, depending on strike point placement and plasma configurations. The photometric calibration of the entire spectrometer system was performed using the Ocean Optics HL-2000 integrating sphere radiometry standard between 800 and 1050 nm.

To aid interpretation of the spectra, the collisional-radiative and radiation transport code CRETIN⁵ was used. The model geometry used a 1 cm slab populated by deuterium plasma at constant T_e and n_e . The deuterium atom model with $n = 1 - 22$ l -resolved levels and atomic rates from Ref.⁶ was used. The background radiation included the continuum (bremsstrahlung) radiation and the free-bound (recombination) radiation. The spectral line

profiles were calculated using the TOTAL code. In profile calculations, Stark broadening due to electron and ion electric microfield, thermal Doppler broadening, and the spectrometer instrumental width were included. In Stark broadening calculations, TOTAL used a quasi-static ion microfield approximation and a binary electron impact collision model. Electric dipole momentum reduced matrix elements calculated elsewhere were used. While radiation transport can strongly affect hydrogen ionization balance, it mostly affects the Lyman series intensities and profiles⁷, so it was not included in these calculations. Zeeman splitting due to DIII-D toroidal field of ~ 3 T was also not included in the present calculations.

III. RESULTS AND DISCUSSION

Survey and line IDs The initial survey of NIR emission in the range 800 – 2300 nm performed in the DIII-D divertor suggests that the NIR spectroscopy can be used for machine protection and plasma control diagnostic applications, as well as for plasma performance evaluation and physics studies². Shown in Fig. 1 is the survey spectrum composed of seven low-resolution uncalibrated spectra taken in seven reproducible 1.2 MA, 2 MW NBI-heated lower- $n_e \simeq 5 \times 10^{19} \text{ m}^{-3}$ discharges. The inner divertor line of sight was used, hence, the emission was representative of the inner divertor far scrape-off layer plasma. Besides the deuterium Paschen series lines $n = 3 - m$, where $m = 4 - 6$, the spectrum contains a large number of neutral and ionized low- Z impurities intrinsic to the tokamak, e.g., B I, C I, C II, and possibly O I. We note that a number of neutral and singly-ionized helium, beryllium and lithium lines are also within the NIR range (as, e.g., observed in NSTX²), however, these elements were not present in the DIII-D divertor. For nearly all of the lines in Fig. 1), ionization per photon (S/XB) and photon emission coefficient (PEC) factors are available in the ADAS database⁸, making them good candidates for recycling, impurity influx, and Doppler measurements. A number of line-free regions could also be suitable for NIR bremsstrahlung measurements for plasma Z_{eff} analysis^{9,10}.

For photometrically calibrated NIR emission analysis, several factors must be carefully considered. One concern for NIR measurements is the parasitic emission from plasma bremsstrahlung and the blackbody (Planck) emission of heated plasma facing components. For the deuterium, as well as the neutral and singly ionized impurities, line emission is strongly localized to the surface. Their emission intensity is typically greater than the NIR

bremsstrahlung of core plasmas, as has been previously discussed². The Planck emission from hot spots can complicate the measurements. The graphite PFC temperature in DIII-D was typically between 300-600 °C, reaching up to 1000 °C during transients.

Emission in the range 1-1.06 μm for Thomson scattering diagnostic applications Measurements and modeling of the intensity and components of background emissions in the spectral range 1-1.06 μm have been recently motivated by the development of the Nd:YAG laser ($\lambda = 1.06 \mu\text{m}$) divertor Thomson scattering diagnostic for ITER¹¹⁻¹³. The components of the emissions, e.g., the blackbody, bremsstrahlung, recombination and impurity lines, including C, N, O, Ne and P7 lines, can significantly contribute to the system noise, hence a validated background emission model for diagnostic performance assurance is needed. The P7 line at $\lambda = 1049 \text{ nm}$ is of particular concern, as it falls within the range actively used for $T_e \leq 100 \text{ eV}$ measurements¹¹.

High resolution NIR spectra were obtained in the DIII-D divertor during high-density operation and during neon seeded operation. The latter may be particularly useful for DTS, as neon may be used in radiative divertor power dissipation in DIII-D and ITER, and experimental tokamak divertor neon NIR spectra have not been previously reported. The intrinsic spectra shown in Fig. 2 are similar to those previously measured in the graphite divertor^{2,11}. They included the deuterium P6, P7 lines and some intrinsic C I and O I lines. Shown in Fig. ?? (c) is the low-resolution neon spectrum obtained by subtracting spectra measured during and before neon seeding in an H-mode discharge. A number of Ne I lines were identified as shown. Some weak lines were identified in the range critical for Nd:YAG DTS system. A stronger multiplet was identified at about $\lambda \simeq 1000 \text{ nm}$, which may be of concern for the measurements of $T_e \geq 200 \text{ eV}$ ¹¹.

The Br9-P α intensity ratio for radiative divertor control. A radiative divertor technique is used in present day tokamak experiments and planned for ITER to mitigate high heat loads on divertor plasma-facing components to prevent their excessive erosion and thermal damage. An inherent characteristic of the radiative diverter is volumetric plasma recombination that provides a mechanism for momentum loss needed for plasma pressure loss (detachment) at the diverter target. Parameters of the detachment process, such as plasma T_e and the extent of recombination region can be used for the diverter detachment process feedback control in real time in order to maintain the desired diverter characteristics, including low T_e , high n_e , and a stable position of the radiation front region at a distance

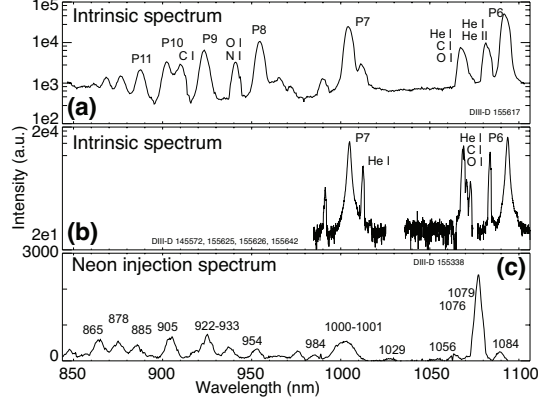


FIG. 2. Intrinsic (a) low-resolution and (b) high-resolution divertor spectra; (b) neon injection divertor spectrum.

from the confined plasmas³.

The hydrogenic series is a very sensitive diagnostic of detached divertor $T_e \leq 0.5 - 2$ eV and $n_e \geq 5 \times 10^{19} \text{ m}^{-3}$ (e.g.,^{1,14}). This is due to the three-body recombination rate R strong sensitivity to local divertor plasma T_e, n_e : $R \sim n_e^3$ and $R \sim T_e^{-4.5}$. The deuterium high- n Balmer series spectra are indicative of recombination rate R and local T_e, n_e , as their upper n -levels are populated by three-body recombination, the populations are governed by the Boltzman distribution, and their Stark broadening is due to electron and ion electric micro-field which can become appreciable at high densities¹⁵ $n_e \geq 5 \times 10^{19} \text{ m}^{-3}$. The extended NIR emission survey revealed for the first time the Brackett series lines Br 7-Br 10. While the present setup lacked the spectral resolution for accurate line broadening measurements, a line intensity ratio between Br9 and $P\alpha$ was considered as a possible T_e -sensitive diagnostic. Since the lines are very close to each other, a photometric calibration could be neglected. The upper levels of the $P\alpha$ $n = 3-4$ line and the Br9 $n = 4-9$ line are strongly populated by by cascades from higher levels and the direct three-body electron-ion recombination capture. One of the cascade channels for $P\alpha$ is the Br9 transition. At low T_e the $P\alpha$ -Br9 intensity ratio is low, whereas if the T_e increases, the recombination rate R strongly decreases, the cascades to $n = 4$ weaken and both line intensities become weak, while their intensity ratio becomes higher. The line intensities are sensitive to both n_e and T_e : their intensity changes by 10^2 over $n_e = 5 \times 10^{19} - 5 \times 10^{20} \text{ m}^{-3}$, and a factor 3-4 over $T_e = 1 - 10$ eV, as shown in Fig. 3 (b). We note, however, that if only line intensities are considered, the Br9/ $P\alpha$

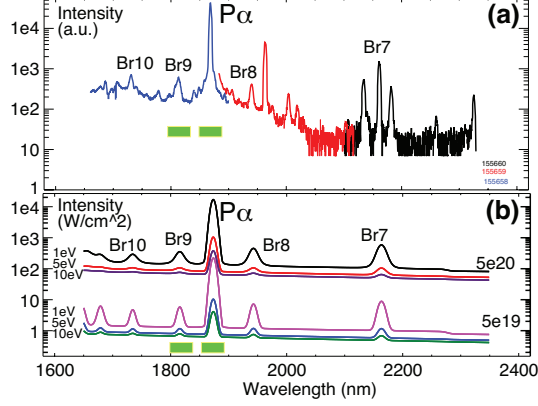


FIG. 3. Deuterium $P\alpha$ and Br7 - Br10 lines measured in the divertor (a), and spectra modeled with the CRETIN code (b).

ratio is T_e sensitive in the 1-3 eV range. The CRETIN calculations are in agreement with the ratio extracted from the recombination photon emission coefficients in ADAS⁸.

A T_e estimator for divertor detachment control can provide bandpass measurements of the line ratio in real time to distinguish between a line-integrated low $T_e \sim 1$ eV region and higher $T_e \geq 5$ eV and provide a control signal for the plasma control system actuator (impurity seeding rate). Commercial InGaAs detectors with bandpass filters linked via a fiber or mirror to imaging telescopes can be used for spatially resolved (spot) T_e evaluation in real time. The bandpass filter integrates both the line emission and the background. The inclusion of the background was found to be beneficial to the Br9/ $P\alpha$ ratio sensitivity to T_e since both the bremsstrahlung and the free-bound continuum spectra are sloped in the NIR range¹. Shown in Fig. 4 is the synthetic diagnostic based on the calculated spectra presented Fig. 3. The ratio of the Br9 and $P\alpha$ bandpass intensities recovers T_e sensitivity in the 1-10 eV range. An example of the measured Br9/ $P\alpha$ bandpass ratios for three DIII-D discharges of different densities are shown in Fig. 4 (b). The ratios indicated a realistic range of divertor $T_e \simeq 1 - 10$ eV. Further work will compare independent T_e measurements from Langmuir probes or DTS to the Br9/ $P\alpha$ ratios for verification of the technique.

In summary, we have assessed three new aspects of the extended NIR spectra measured for the first time in the DIII-D divertor. The first full NIR survey supports measurements of plasma T_e , n_e , and impurity fluxes for plasma-surface interaction studies. The range 1.000-1.060 μm was surveyed during high-density and neon seeded divertor operation for divertor

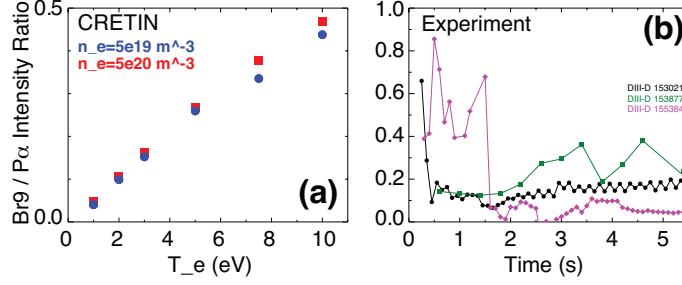


FIG. 4. Calculated (a) and measured (b) $\text{Br9}/\text{P}_\alpha$ ratio.

Thomson scattering diagnostic system development. The ratio of deuterium Brackett Br9 and Paschen- α lines was shown to be suitable for divertor T_e estimates aimed at divertor detachment feedback control.

ACKNOWLEDGMENTS

The authors would like to thank the entire DIII-D Team for plasma and diagnostic operations. Dr. H. Scott (LLNL) is acknowledged for the CRETIN code. The ARC spectrograph used in this work was on loan from Princeton Plasma Physics Laboratory. This work was supported by the US Department of Energy under DE-AC52-07NA27344 and DE-AC02-09CH11466. The data shown in figures is from the DIII-D tokamak.

REFERENCES

- ¹V. Soukhanovskii, D. Johnson, R. Kaita, and A. Roquemore, Rev. Sci. Instrum. **77**, 10127 (2006).
- ²V. Soukhanovskii, Rev. Sci. Instrum. **79**, 10539 (2008).
- ³V. Soukhanovskii, S. Gerhardt, R. Kaita, A. McLean, and R. Raman, Rev. Sci. Instrum. **83**, 10 (2012/10/).
- ⁴D. Hill and the DIII-D Team, Nuclear Fusion **53**, 104001 (2013).
- ⁵H. Scott, J. Quant. Spectrosc. Radiat. Transf. **71**, 689 (2001).
- ⁶L. Johnson and E. Hinnov, J. Quant. Spectrosc. Radiat. Transf. **13**, 333 (1973).
- ⁷H. Scott, A. Wan, D. Post, M. Rensink, and T. Rognlien, J. Nucl. Mater. **266**, 1247 (1999).

- ⁸H. P. Summers, The ADAS User Manual, version 2.6 <http://adas.phys.strath.ac.uk> (2014).
- ⁹K. H. Steuer, H. Rohr, and B. Kurzan, Rev. Sci. Instrum **61**, 3085 (1990).
- ¹⁰F. Orsitto, M. R. Belforte, A. Brusadin, E. Giovannozzi, D. Pacella, and M. J. May, Rev. Sci. Instrum **70**, 926 (1999).
- ¹¹S. Tolstyakov, E. Mukhin, M. Kochergin, G. Kurskiev, V. Semenov, A. Razdobarin, K. Podushnikova, A. Zabuga, V. Lisitsa, M. Levashova, V. Soukhanovskii, M. Beurskens, S. Brezinsek, A. Meigs, and P. Andrew, J. Phys., Conf. Ser. **227**, 012045 (2010).
- ¹²V. S. Lisitsa, E. E. Mukhin, M. B. Kadomtsev, A. B. Kukushkin, A. S. Kukushkin, G. S. Kurskiev, M. G. Levashova, and S. Y. Tolstyakov, Plasma Physics Reports **38**, 138 (2012).
- ¹³E. Mukhin, R. Pitts, P. Andrew, I. Bukreev, P. Chernakov, L. Giudicotti, G. Huijsmans, M. Kochergin, A. Koval, A. Kukushkin, G. Kurskiev, A. Litvinov, S. Masyukevich, R. Pasqualotto, A. Razdobarin, V. Semenov, S. Tolstyakov, and M. Walsh, Nucl. Fusion **54**, 043007 (2014).
- ¹⁴B. Welch, H. Griem, J. Weaver, J. Brill, J. Terry, B. Lipschultz, D. Lumma, G. McCracken, S. Ferri, A. Calisti, R. Stamm, B. Talin, and R. Lee, AIP Conf. Proc. **386**, 113 (1997).
- ¹⁵H. R. Griem, Phys. Scripta **T83**, 142 (1999).